Desalination and Water Treatment
www.deswater.com

doi:10.5004/dwt.2017.21517

94 (2017) 31–39
October

Removal of fluoride ions by calcium hydroxide-modified iron oxides

J.J. García-Sánchez[a], M. Solache-Ríos[b,*], V. Martínez-Miranda[c], I. Rodriguez-Torres[d]

[a]*Tecnológico de Estudios Superiores de Jocotitlán, Carretera Toluca-Atlacomulco Km 44.8, Ejido de San Juan y San Agustín Jocotitlán, 50700 Jocotitlán, México, email: jjuangs@gmail.com*
[b]*Departamento de Química, Instituto Nacional de Investigaciones Nucleares, Carr. México-Toluca S/N (km. 36.5), 52750 Estado de México, Mexico, Tel. +52 5553297200x2271, Fax +525553297301, email: marcos.solache@inin.gob.mx*
[c]*Centro Interamericano de Recursos del Agua, Facultad de Ingeniería, Universidad Autónoma del Estado de México, Km. 14.5, Carretera Toluca-Ixtlahuaca, Toluca, Estado de México, México, email: mmirandav@uaemex.mx*
[d]*Instituto de Metalurgia, Facultad de Ingeniería, Universidad Autónoma de San Luis Potosí, Av. Sierra Leona 550, lomas 2[a] sección, 78210 San Luis Potosí, SLP, México, email: learsi@uaslp.mx*

Received 15 February 2017; Accepted 6 October 2017

ABSTRACT

Untreated and modified iron oxides from steel pipes of a drinking water distribution system have been used to remove fluoride ions from water. In this work the behavior of fluoride ions in the presence of calcium hydroxide-modified iron oxides was evaluated to determine how the fluoride ions could be removed by this material. The adsorption of fluoride ions was studied in a batch system using hydroxide-modified iron oxides (CP-Ca), and the adsorption capacity was determined. The effects of pH, contact time, and the dose of sorbent on the adsorption of fluoride ions were considered. The point of zero charge (PZC) was 12.25; there were more basic sites than acid sites in the calcium-hydroxide-modified iron oxides. The adsorbent showed a maximum adsorption yield value of 76% from a 5 mg/L fluoride solution at pH 10 and a maximum adsorption capacity of 0.55 mg/g. The adsorption equilibrium was reached in 48 h, and the kinetic and isotherm data were adjusted to the pseudo-second order and Freundlich models, which indicated a chemisorption mechanism on a heterogeneous material.

Keywords: Fluoride removal; Iron oxides-calcium hydroxide; Surface precipitation; Adsorption; Desalination; Drinking water; Groundwater

1. Introduction

Fluoride pollution of water occurs through natural sources and anthropogenic facilities. Since fluoride is present in minerals and geochemical deposits, it is generally released into groundwater sources by the slow natural degradation of fluorine in rocks [1]. Excessive fluoride in groundwater is found in many regions worldwide. Many groundwater wells in the north-central part of Mexico contain fluoride in concentrations higher than 6 mg/L [2]. However, the maximum acceptable concentration of fluoride in drinking water established by the World Health Organization is 1.5 mg/L [3].

Various health problems have been associated to excessive fluoride exposure, including dental, skeletal, and non-skeletal fluorosis. Dental fluorosis only occurs during tooth formation and becomes apparent upon eruption of teeth. Skeletal fluorosis is caused by a complex dose-related action of fluoride on bone. As a result of these effects, bone changes are observed in people exposed to high levels of fluoride [4]. Fluoride can affect non-calcified tissues besides bone and teeth, which is called non-skeletal fluorosis. The soft tissue organs that can be affected by fluoride are the aorta, thyroid, lungs, kidneys, heart, pancreas, brain, and spleen [5].

Fluoride removal from aqueous solutions can be achieved by several methods including coagulation/

*Corresponding author.

precipitation [6], electrocoagulation [7], fluidized-bed crystallization [8], and adsorption/ion exchange [9,10]. Adsorption is one of the most important methods for water defluoridation. Many adsorbents have been used to remove fluoride from aqueous solutions and water. Such materials include alumina and aluminum (acidic alumina) [11], amorphous $Al(OH)_3$, and gibbsite or alumina (Al_2O_3) [12], iron-based adsorbents (polypyrrole (PPy)/Fe_3O_4 magnetic nanocomposites [13], amorphous Fe/Al mixed hydroxides [14], granulated mixture of Fe-Al-Ce nano adsorbent [15], natural stilbite zeolite modified with Fe(III) [16], iron-impregnated granules ceramics [17], granular ferric hydroxide [18], synthetic siderite [19], Mg-doped nano ferrihydrite powder [20], Fe(III) modified montmorillonite [21], and iron rich laterite [22], calcium-based adsorbents (crushed limestone) [23], aluminum hydroxide impregnated limestone [24], apatitic tricalcium phosphate [25], calcium phosphate minerals [26], calcium aluminate [27], metal oxides/hydroxides/oxyhydroxides (CeO_2-TiO_2/SiO_2) [28], magnesia-amended silicon dioxide granules [29], nanosized superparamagnetic zirconia material (ZrO_2/SiO_2/Fe_3O_4) [30], Al-Ce hybrid adsorbent [31], gel like titanium hydroxide derived adsorbent from titanium oxysulfate $TiO(SO_4)$ [32], aluminum titanate and bismuth aluminate [33], magnesia (MgO) and magnesia/chitosan (MgOC) [34], calcined magnesia with pullulan [35], aluminum and zirconium oxide [36], magnesium titanate [37], bauxite [38], and Mn-Ce oxide [39], bio adsorbents [40], neodymium-modified chitosan [26], carboxylated chitosan beads [27], lanthanum incorporated chitosan beads [41], chitin or a chitin-based biocomposite [29], rice husk ash coated with aluminum hydroxide [30], and carbon-based sorbents (multi-walled carbon nanotubes) [42], modified carbon with aniline-co-o-aminophenol [31], fishbone charcoal [32], zirconium impregnated activated charcoals [33], granular activated carbon coated with manganese oxides [35], graphite [36], carbons loaded with specific chemical moieties prepared from pecan nut shells employing a natural modifier agent obtained from egg shell [37], graphene [38], cerium dispersed in carbon, a hybrid sorbent prepared by carbonization of ammonium cerium sulfate impregnated starch [10], carbon from acacia Arabica fruit [39], activated carbon from biomaterials of bergera koenigh [curry leaf seeds], batavia orange and raphanus sativus [garden radish] [43].

Iron oxides from steel pipes of a drinking water system have shown some capacity to remove fluoride ions, which is interesting because some fluoride ions may be removed during water distribution [44]. Hard water contains mainly calcium and magnesium, and these ions dissolve when water is in contact with minerals such as limestone, chalk, and dolomite. In a previous work the presence of magnesium in these oxides was evaluated for the removal of fluoride ions [45]. The novelty of this paper is the determination of the behavior of fluoride ions in the presence of the corrosion products formed in the drinking water distribution systems and calcium which is present in hard waters. Therefore, the aim of this paper was to determine the surface precipitation behavior of fluoride ions on hydroxide-modified iron oxides (iron oxides from steel pipes of a drinking water system). Experimental parameters such as pH, contact time, point of zero charge, and active surface sites were considered.

2. Experimental

2.1. Materials and solutions

Iron oxide from a steel pipe corrosion products (CP) formed in a drinking water distribution system were used in this work; the oxides were crushed and sieved following the method introduced elsewhere [45] particle sizes between 80 and 100 meshes (0.180 and 0.150 mm) were chosen. The characterization of the CP by X-ray diffraction has been reported elsewhere [44] and the main components of the corrosion products were magnetite, lepidocrosite, hematite, geotite, and ferrous oxide, which are found in the layers of corrosion formed in hydraulic systems [47]. Solutions of 5 mg F^-/L and pH 6.5 were prepared from a standard sodium fluoride solution of 100 mg F^-/L (Thermo Fisher Scientific, USA). Distilled water was used to prepare all solutions.

2.2. Modifications of CP with $CaCl_2$

Calcium hydroxide was obtained by adding a 2 M KOH (ACS reagent, ≥97.0%, pellets, Sigma-Aldrich) solution to a 0.1 M calcium chloride (99.99% trace metals basis, Sigma-Aldrich) solution up to a pH of 12.5, the precipitate was washed 3 times with distilled water. The calcium hydroxide was mixed with the CP in distilled water, the mixture was shaken for 4 h, and finally, the water was decanted and the material was dried at 50°C for 5 h. The sample was labeled as CP-Ca.

2.3. Characterization of the CP-Ca

2.3.1. Scanning electron microscopy

The corrosion products were mounted directly on the holders and then observed at 10 and 20 kV in a JEOL JSM-5900-LD electron microscope. The microanalysis was done with an energy X-ray dispersive spectroscopy (EDS) system.

2.3.2. Determination of point of zero charge

The points of zero charge of CP and CP-Ca were determined by the following process [48]: 0.1 N HCl and NaOH solutions were prepared, then volume aliquots (0.1, 0.2, 0.4, 0.6, 0.8, 1.0, 1.5, 2.0, 3.0, 4.0, and 5.0 mL) of each solution were put in volumetric flasks and adjusted to 50 mL with a 0.1 N NaCl solution. Next, 0.1 g of each adsorbent (CP or CP-Ca) was left with 25 mL of each solution (nitrogen was bubbled through the mixtures) for 48 h, and the other 25 mL samples were left without any adsorbent. Then the pH of each solution was measured.

2.3.3. Determination of surface acidity and basicity

Both the surface acidity and basicity of CP-Ca were determined by a titration method reported by Moreno-Castilla et al. [49] and Guze[50]. The CP-Ca sample was sieved

through a 100 mm sieve, washed several times with distilled water, and then dried at 100°C for 24 h prior titration.

2.3.4. Surface acidity

1 g of CP-Ca was prepared as described above and put into contact with 50 mL of a 0.01 N NaOH solution; the sample was shaken at 25°C for 5 days using an automatic shaker, then the mixture was filtered and an aliquot (10 mL) of the supernatant was back-titrated with a 0.01 N HCl solution. The concentrations of acidic and basic groups on the surface were determined and expressed as meq/g.

2.3.5. Surface basicity

The total surface basicity of the CP-Ca was quantified by mixing 1 g of the adsorbent with 50 mL of a 0.1 N HCl solution; the mixture was shaken for 5 days at 25°C. The mixture was filtered and an aliquot (10 mL) of the supernatant back-titrated with a 0.1 N NaOH solution.

2.4. Fluoride measurements

The fluoride concentrations in the remaining solutions were measured with a specific ion electrode (ISE301F) by using a total ionic strength adjustment buffer (TISAB) solution to eliminate the interference of complexing ions.

2.5. Batch experiments

Batch experiments were carried out by putting in contact 10 mL aliquots of fluoride solution (5 mg/L) and 0.1 g of the adsorbent. The samples were shaken at 45 rpm for 48 h at 30°C, then the mixtures were separated and fluoride ions were measured in the remaining solutions, as described above; each experiment was done in duplicate. The removal efficiency of fluoride ions and equilibrium adsorption capacities were obtained by the following equations:

$$n = \frac{C_o - C_e}{C_o} \times 100\% \quad (1)$$

$$q_e = \frac{V(C_o - C_e)}{W} \quad (2)$$

where n (%) is the removal efficiency of fluoride ions; q_e the equilibrium adsorption (mg/g) in the solid at equilibrium; C_o and C_e are the initial and equilibrium concentrations of fluoride ions (mg/L), respectively; V (L) is the volume of the aqueous solution; and W is the mass (g) of adsorbent used in the experiments.

The quantities of adsorbents used to determine the effect of sorbent dose were 10, 20, 40, 60, 80, 100, 120, 140, 160, 180, and 200 mg. The contact times considered for the adsorption kinetics were 0.83, 0.25, 0.5, 1, 3, 5, 7, 24, 48, and 72 h, and the effect of pH on the adsorption of fluoride ions was determined from initial pH from 2 to 12.

3. Results and discussion

3.1. Scanning electron microscopy

Fig. 1 shows the morphology of the corrosion products before and after treatment with calcium hydroxide, some aggregates are observed; these dispersed aggregates correspond to the top surface layer of the corrosion products [44]. The chemical compositions of the corrosion products are presented in Table 1; iron, oxygen, carbon, silicon, aluminum, sulfur, manganese, calcium, phosphorus, magnesium, potassium, and chlorine were found in the sample (potassium and chloride have high standard deviations, indicating that the distribution in the sample is heterogeneous), and the most abundant elements were iron, oxygen, and carbon. Some elements found correspond to additional products of the oxidation of iron, including precipitation products such as carbonates, silicates, sulfates, and chlorides. The calcium concentration increased after treatment, and some other elements present may come from the treatment of drinking water.

3.2. Point of zero charge (PZC)

The PZC values of the unmodified and modified adsorbent were determined by plotting the pH of the solution against the volume of the titrating solution and the pH

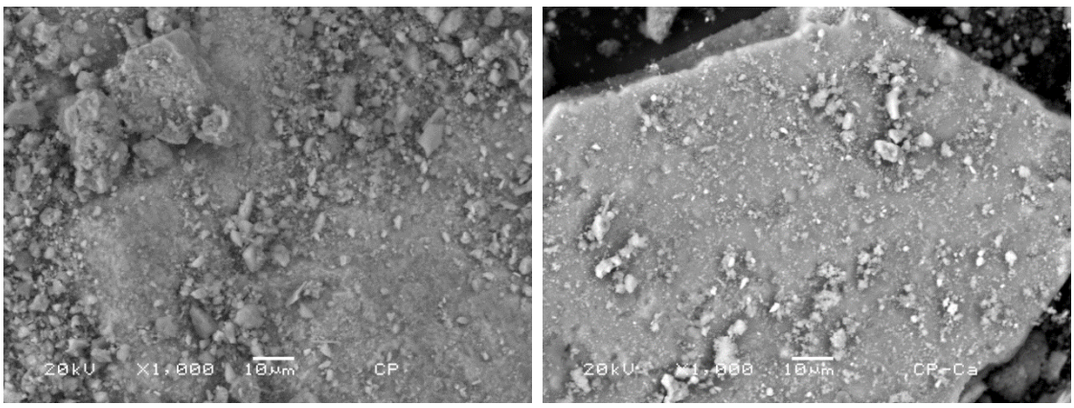

Fig. 1. Corrosion products morphologies before (left) and after treatment with calcium (right).

Table 1
Elemental analysis of CP and CP-Ca by EDS

Element	CP	CP-Ca
C	12.53±6.13	16.74±8.56
O	32.27±2.87	24.83±15.53
Mg	0.19±0.12	–
Al	0.46±0.09	1.23±1.06
Si	3.19±0.71	0.79±0.49
P	0.62±0.18	–
S	0.13±0.05	–
Cl	–	8.43±12.81
K	–	7.59±14.08
Ca	0.62±0.14	11.96±8.16
Mn	0.69±0.42	–
Fe	49.27±4.52	28.40±21.26

where these two curves intercept corresponds to the PZC. The values were 7.87 and 12.25 (Figs. 2 and 3), respectively. The materials are positively charged when the pH is lower than the PZC and negatively charged when it is higher than the PZC. The PZC of the modified adsorbent is basic; this suggests that the calcium hydroxide modification introduce hydroxyl groups and there is a higher proportion of basic sites than acid sites.

3.3. Determination of active sites

The curves obtained from the determination of acid and basic sites for the modified and unmodified adsorbent are shown in Figs. 4 and 5, respectively. It is observed that CP-Ca has more basic sites than acid sites and at the same time has a lower quantity of acid groups than the unmodified material. It can be seen that the modification causes an increase in the amount of basic groups in the adsorbent (Fig. 4), and these active surface sites favor the surface precipitation of fluoride ions. Table 2 shows active sites concentrations of CP and CP-Ca.

3.4. Adsorption

3.4.1. Effect of contact time

The effect of contact time on fluoride uptake by CP-Ca is shown in Fig. 6. Fluoride adsorption increased from 53 to 75% as the time increased from 1 h to 48 h. The fluoride adsorption was fast at the beginning and then became slow until equilibrium was reached. The adsorption was probably a result of exchange of fluoride ions with hydroxyl ions on the surface of the adsorbent.

Pseudo-first and pseudo-second order kinetics models were used to treat the experimental data. In general, the best fit of the experimental data was observed with the pseudo-second order model, which indicates adsorption on a heterogeneous material involving chemical reactions.

The linear form of the model can be represented by the following equation [51]:

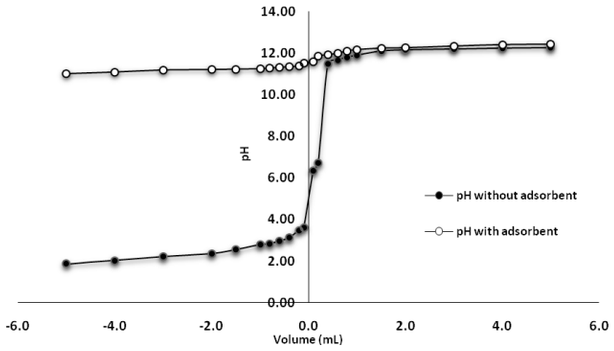

Fig. 2. Point of zero charge of the modified adsorbent (CP-Ca).

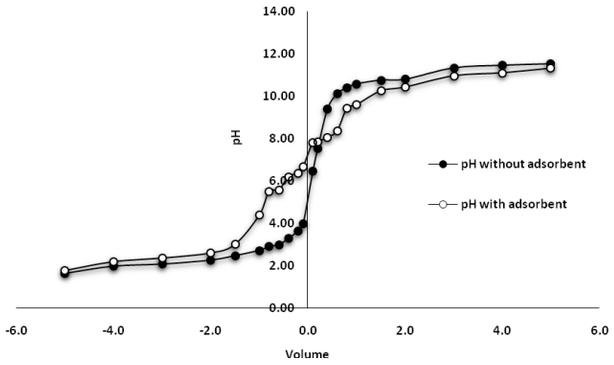

Fig. 3. Point of zero charge (PZC) of the unmodified adsorbent (CP).

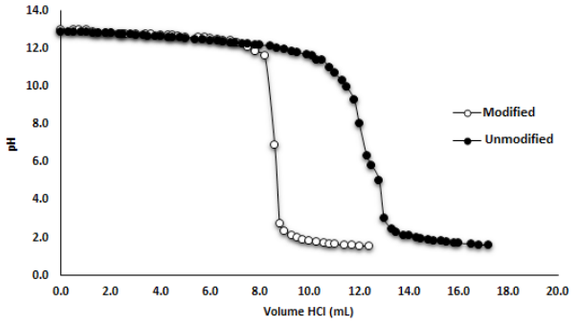

Fig. 4. Acid sites of the modified and unmodified adsorbent.

$$\frac{t}{q_t} = \frac{1}{Kq_e^2} + \frac{t}{q_e} \quad (3)$$

where K (g/mg min) is a constant of the pseudo-second order, q_t (mg/g) is the amount of fluoride ions adsorbed at time t, and q_e (mg/g) is the amount of fluoride ions adsorbed at equilibrium.

The calculated q_e from the fitting of experimental data to the pseudo-second order model and the experimental one for the adsorption of fluoride ions by CP-Ca were 0.38 and 0.37 mg F^-/g, respectively. The value of K was 2.98 g/mg h with an R^2 of 0.9991. The adsorption capacity of CP-Ca

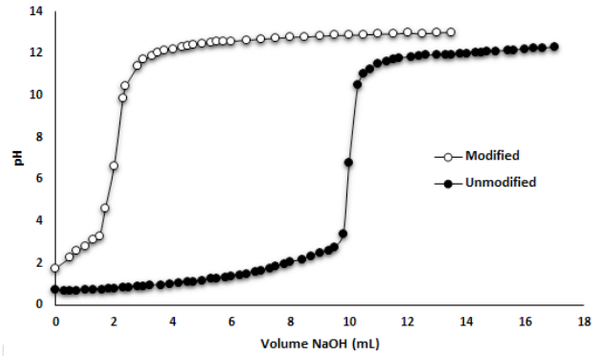

Fig. 5. Basic sites of the modified and unmodified adsorbent.

Table 2
Active sites concentrations of CP and CP-Ca

Adsorbent	Active sites, (meq/g)	
	Total acid	Total Basic
CP	1.4	0.1
CP-Ca	0.7	4.0

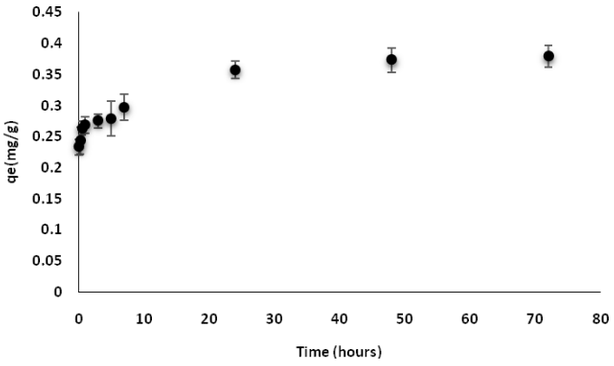

Fig. 6. Removal of fluoride as a function of time, (dosage of sorbent: 10 g/L, initial concentration: 5 mg/L, pH: 12.0, temperature: 30°C, shaking speed: 400 rpm).

is higher than the value reported for aluminum hydroxide (0.11 mg/g) [52].

3.4.2. Effect of pH

The pH is an important parameter that generally controls adsorption processes, it plays an important role on the amount of fluoride removed from solution because of the ionization of surface functional groups and the chemical composition of solution. Fig. 7 shows the fluoride ion adsorption capacities of CP-Ca at various pH values and at room temperature. The results show that maximum adsorption capacity occurred in the pH range from 10 to 12, the exchange between the hydroxide groups and the F^- may be responsible for this behavior, the adsorption capacity showed a gradual increase with increasing

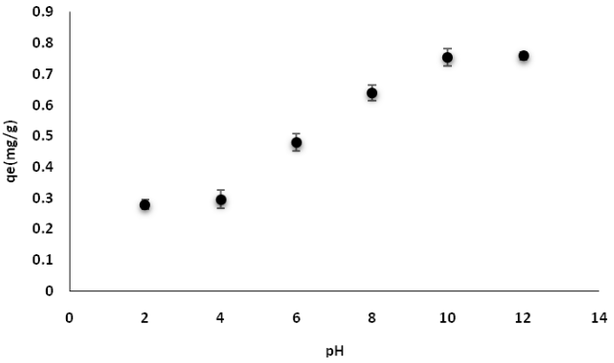

Fig. 7. Effect of pH on removal efficiency of F^- (dosage of sorbent 10 g/L; initial concentration: 5 mg/L; contact time 24 h; shaking speed: 400 rpm and 30°C).

pH. The adsorption is similar at pH 2 and 4, and then it increases up to pH 10, a similar behavior to the content of basic sites (Figs. 4 and 5); this indicates that the adsorption increases as the number of basic sites increases. At a low pH (pH<4), gaseous HF is formed that gradually escapes from the solution, and measurement of fluoride ions is difficult in these conditions. Fluoride ions are the predominant species at pH>4, and precipitation on the material in alkaline conditions may occurs. In these conditions fluoride ions are incorporated on the surface by ion exchange, and calcium may react with fluoride ions at pH between 10 and 12.

3.4.5. Effect of sorbent dose

The effect of sorbent dose on fluoride adsorption at pH 6.5 and the initial fluoride concentration of 5 mg/L is shown in Fig. 8. As shown in this figure, the adsorption capacities of CP-Ca for fluoride ions decrease as the sorbent dosage increases. The corresponding isotherm is shown in Fig. 9; the data obtained were fitted to Langmuir and Freundlich models [51, 53], and the results are shown in Figs. 10, 11 and Table 3, the maximum adsorption capacity determined from the experimental data and Langmuir model was 0.55 mg/g. The Freundlich isotherm has a higher correlation coefficient R^2 value than the Langmuir isotherm, which indicates that CP-Ca is a heterogeneous material. This behavior was expected because a plateau is not observed in the isotherm (Fig. 9).

The surface of CP contains goethite (α-FeOOH) and lepidocrocite (γ-FeOOH) among others [44], both compounds may interact with Ca^{2+} ions to form cationic complexes $FeOOCa^+$ [54] as shown in Fig. 12A, adsorption of calcium cations onto iron oxides may be described by surface complexation models, and substitution of calcium for hydrogen is assumed to be given by a surface coordination reaction [55]. These chemical species are active sites that can interact with the fluoride ions(Fig. 12B). The surface precipitation may occur when calcium ions or other ions like aluminum, magnesium, or lanthanum are added to the iron oxides.

Table 4 shows a comparison of the kinetic adsorption efficiencies of fluoride ions by modified corrosion

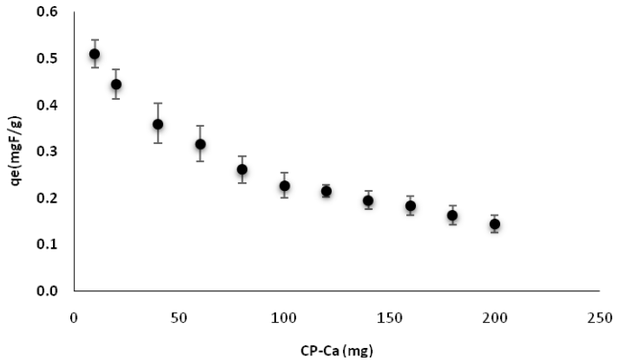

Fig. 8. Effect of the sorbent dosage on the fluoride ions adsorption.

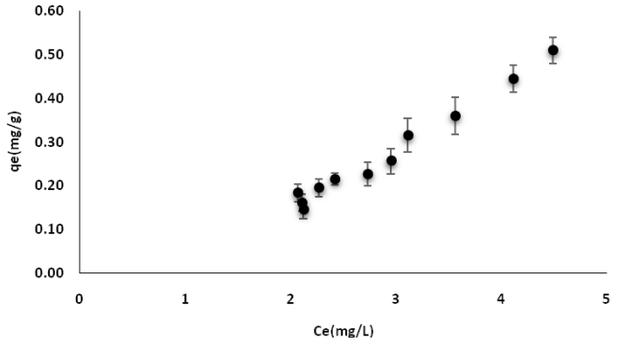

Fig. 9. Isotherms model of fluoride ions adsorption from fluoride solutions.

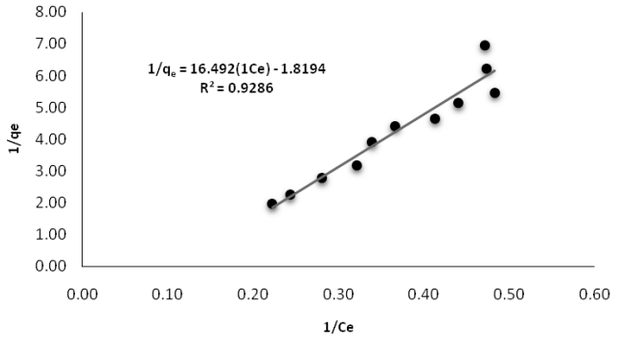

Fig. 10. Langmuir isotherms applied to the fluoride ions adsorption from aqueous solution by CP-Ca.

products formed in a drinking water distribution system. Corrosion products from cast iron pipes and stainless steel pipes have been studied, the efficiency of fluoride removal depends on the materials used in the distribution systems. Corrosion products from cast iron pipes are more efficient to remove fluoride ions from water than corrosion products from stainless steel pipes, as shown in Table 4. Lanthanum-modified corrosion products show the highest adsorption capacity, followed by aluminum- and calcium-hydroxide-modified materials. The adsorption capacities were similar for the last two materials, which could be attributed to the similar modification processes. It is important to note that the adsorption properties of the materials depend on the modification process; the corrosion products were modified with calcium sulfate without adding a basic solution to increase the pH, and the adsorption of fluoride ions by the resulting material was very poor (0.02 mg/g) [46]. In this work, calcium modification was similar to the procedure reported with aluminum [46]; a basic solution was added in both cases to form the hydroxides, and the adsorbents showed the same adsorption capacities (0.38 mg/g). The lowest fluoride adsorption capacity obtained for CP_2-Mg may be attributed to the low affinity between CP-Mg and fluoride ions. These results indicate that the fluoride content in drinking water may be reduced by the corrosion products formed in the distribution system of drinking water, and the presence of calcium may improve removal efficiency.

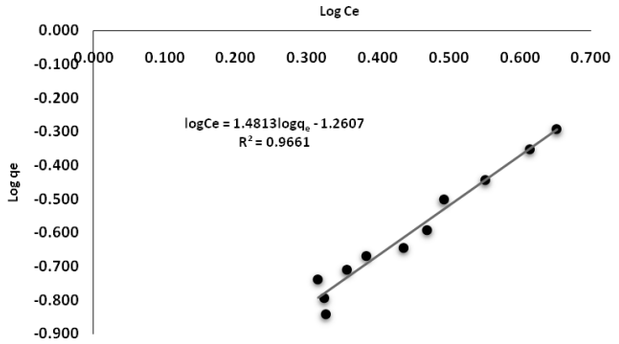

Fig. 11. Freundlich isotherms applied to the fluoride ions adsorption from aqueous solution by CP-Ca.

Table 3
Isotherm models applied to the fluoride ions adsorption from aqueous solutions

Models	Equations	Fluoride ion solution (5 mg/L)
Langmuir	$\frac{1}{q_e} = \frac{1}{Q^0} + \frac{1}{bQ^0C_e}$	$Q^0 = 0.55$ mg/g $b = 0.11$ $R^2 = 0.9286$
Freundlich	$\log q_e = \log K_f + \frac{1}{n}\log C_e$	$K_f = 18.23$ $n = 0.68$ $R^2 = 0.9661$

4. Conclusions

The ability of calcium hydroxide-modified iron oxides to adsorb fluoride ions was determined. The capacity of iron oxides to adsorb fluoride ions depends on the metal used in the modification; according to the literature and the results of this work, the adsorption capacity is highest for lanthanum, then for calcium hydroxide and aluminum, and lowest for magnesium. The results showed that the maximum adsorption capacity of calcium hydrox-

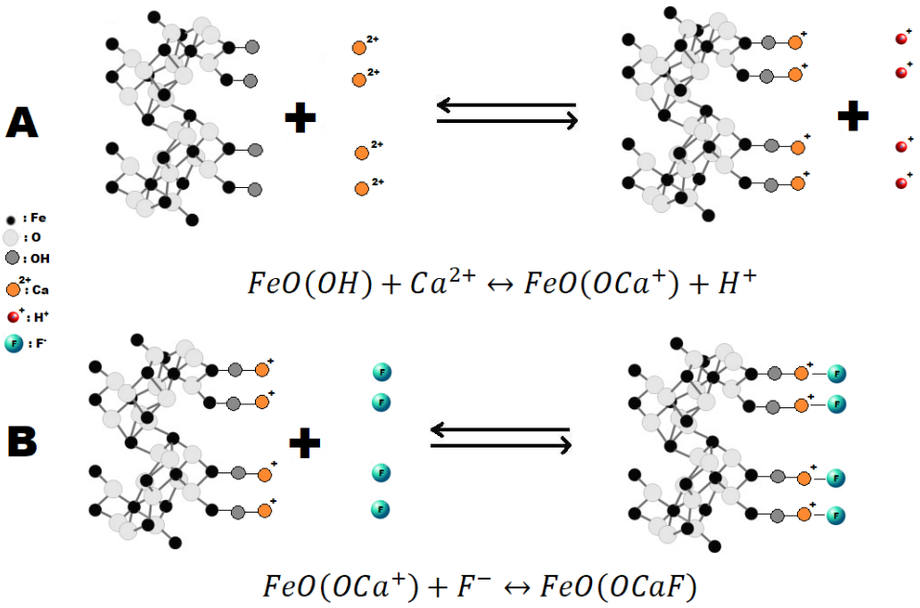

Fig. 12. Schematic representation of surface precipitation of the fluoride ions on CP-Ca.

Table 4
Kinetic fluoride adsorption capacities of untreated and modified CP

Adsorbent	$C_{initial}$ mg/L	$q_{e,exp}$ mg/g	References
CP_1	5	0.44	44
CP_2	5	0.23	46
CP_2-Al	4	0.38	46
CP_2-$Ca_{ion\ exchange}$	4	0.02	46
CP_2-Mg	5	0.20	45
CP_2-La	5	0.47	45
CP_2-$Ca_{precipitation}$	5	0.38	Present work

CP_1 = Corrosion products from cast iron pipe
CP_2 = Corrosion Products from stainless steel pipe
$C_{initial}$ = Initial concentration of fluoride ions

ide-modified iron oxides was in the pH range from 10 to 12. The adsorption capacity showed a gradual increase with the increase of pH; this behavior could be attributed to the formation of hydroxides in alkaline conditions, then the adsorption behavior depends on the modification process. The basic sites were higher than the acid sites for the iron oxides-calcium hydroxide, and the point of zero charge (PZC) was 12.25. The adsorbent showed a maximum defluoridation capacity of 76% from a 5 mg/L fluoride solution at pH 10. The adsorption equilibrium was reached in 48 h, and the kinetic and isotherm data were adjusted to the pseudo-second order and Freundlich models, indicating a chemisorption mechanism on a heterogeneous material. The adsorption capacity was 0.55 mg/g from Langmuir isotherm using a fluoride solution of 5 mg/L. Adsorption properties of iron oxides depend on the modification process and on the metal used for modification. Iron oxides modified with calcium hydroxide show an adsorption capacity 18 times higher than that of the material modified by ion exchange. Fluoride ions may be removed from water solutions by calcium hydroxide-modified iron oxides.

Acknowledgments

We acknowledge financial support from SEP-PRODEP, project 197241.

References

[1] W.M. Edmunds, P.L. Smedley, Groundwater geochemistry and health: an overview, in: Appleton, Fuge, McCall (Eds.), Environmental Geochemistry and Health, Geological Society Special Publication, 113 (1996) 91–105.
[2] C. Diaz-Nava, M.T. Olguin, M. Solache-Rios, Water defluoridation by Mexicanheulandite-clinoptilolite, Sep. Sci. Technol., 37 (2002) 3109–3128.
[3] WHO (World Health Organization). Fluoride in Drinking-water, K. Bailey, J. Chilton, E. Dahi, M. Lennon, P. Jackson, J. Fawell, eds., 2006.
[4] Buzalaf MAR. (Ed.). Fluoride and the Oral Environment. P DenBesten, W. Li Chronic fluoride toxicity: dental fluorosis. Monogr. Oral Sci., 22 (2011) 81–98.
[5] J.A. Alvarez, K.M.P.C. Rezende, S.M.S. Marocho, Dental fluorosis: exposure, prevention and management, Medicina Oral Patologia Oral Cirugia Bucal., 14 (2009) E103–E107.
[6] M.F. Chang, J.C. Liu, Precipitation removal of fluoride from semiconductor wastewater, J. Environ. Eng. ASCE., 133 (2007) 419–425.

[7] C.Y. Hu, S.L. Lo, W.H. Kuan, Simulation the kinetics of fluoride removal by electrocoagulation (EC) process using aluminum electrodes, J. Hazard. Mater., 145 (2007) 180–185.
[8] R. Aldaco, A, Garea, A. Irabien, Calcium fluoride recovery from fluoride wastewater in a fluidized bed reactor, Water Res., 41 (2007) 810–818.
[9] V. Sivasankar, S. Murugesh, S. Rajkumar, A. Darchen, Cerium dispersed in carbon (CeDC) and its adsorption behavior: a first example of tailored adsorbent for fluoride removal from drinking water, Chem. Eng. J., 214 (2013) 45–54.
[10] S.S. Tripathy, J.L. Bersillon, K. Gopal, Removal of fluoride from drinking water by adsorption onto alum-impregnated activated alumina, Sep. Purif. Technol., 50 (2006) 310–317.
[11] M.M. Emamjomeh, M. Sivakumar, A.S. Varyani, Analysis and the understanding of fluoride removal mechanisms by an electrocoagulation/flotation (ECF) process, Desalination, 275 (2011) 102–106.
[12] M.G. Sujana, G. Soma, N. Vasumathi, S. Anans, Studies on fluoride adsorption capacities of amorphous Fe/Al mixed hydroxides from aqueous solutions, J. Fluorine Chem., 130 (2009) 749–754.
[13] P. Zhu, H. Wang, B. Sun, P. Deng, S. Hou, Y. Yu, Adsorption of fluoride from aqueous solution by magnesia-amended silicon dioxide granules, J. Chem. Technol. Biotech., 84 (2009) 1449–1455.
[14] Q. Guo, E.J. Reardon, Fluoride removal from water by meixnerite and its calcination product, Appl. Clay Sci., 56 (2012) 7–15.
[15] H. Liu, S. Deng, Z. Li, G. Yu, J. Huang, Preparation of Al-Ce hybrid adsorbent and its application for defluoridation of drinking water, J. Hazard. Mater., 179 (2010) 424–430.
[16] T. Wajima, Y. Umeta, S. Narita, K. Sugawara, Adsorption behaviour of fluoride ions using a titanium hydroxide-derived adsorbent, Desalination, 249 (2009) 323–330.
[17] M. Karthikeyan, K.P. Elango, Removal of fluoride from water using aluminium containing compounds, J. Environ. Sci., 21 (2009) 1513–1518.
[18] C.S. Sundaram, N. Viswanathan, S. Meenakshi, Defluoridation of water using magnesia/chitosan composite, J. Hazard. Mater., 163 (2009) 618–624.
[19] J. Kang, B. Li, J. Song, D. Li, J. Yang, W. Zhan, D. Liu, Defluoridation of water using calcined magnesia/pullulan composite, Chem. Eng. J., 166 (2011) 765–771.
[20] V. Gopal, K.P. Elango, Studies on defluoridation of water using magnesium titanate, Ind. J. Chem. Tech., 17 (2010) 28–33.
[21] M.G. Sujana, S. Anand, Fluoride removal studies from contaminated ground water by using bauxite, Desalination, 267 (2011) 222–227.
[22] F. Jamasbian, S.J. Attar, D.R. Saini, Defluoridation of water using bauxite adsorbent, Int. J. Eng. Res. Ind. Appls., 2 (2009) 247–257.
[23] V. Sivasankar, T. Ramachandramoorthy, A. Darchen, Manganese dioxide improves the efficiency of earthenware in fluoride removal from drinking water, Desalination, 272(1–3) (2011) 179–186.
[24] N. Lakshminarayan, A.G. Davangere, Evaluation of the water defluoridating potential of brushite-calcite and two indigenous bioadsorbent materials, Fluoride, 44 (2011) 27–29.
[25] G. Alagumuthu, V. Veeraputhiran, R. Venkataraman, Fluoride sorption usingn cynodon dactylon based activated carbon, Hem. Ind., 65 (2011) 23–35.
[26] R. Yao, F. Meng, L. Zhang, D. Ma, M. Wang, Defluoridation of water using neodymium-modified chitosan, J. Hazard. Mater., 165 (2009) 454–460.
[27] N. Viswanathan, C. Sundaram, S. Meenakshi, Development of multifunctional chitosan beads for fluoride removal, J. Hazard. Mater., 167 (2009) 325–331.
[28] S.V. Ramanaiah, S.V. Mohan, P.N. Sarma, Adsorptive removal of fluoride from aqueous phase using waste fungus (Pleurotus ostreatus 1804) biosorbent: Kinetics evaluation, Ecol. Eng., 31 (2007) 47–56.
[29] J.L.D. Rodríguez, A. Vladimir, E. Barrios, J.R.R. Méndez, Removal of fluoride from drinking water by a chitin-based biocomposite in fixed-bed columns, J. Fluorine Chem., 140 (2012) 99–103.
[30] V. Ganvir, K. Das, Removal of fluoride from drinking water using aluminum hydroxide coated rice husk ash, J. Hazard. Mater., 185 (2011) 1287–1294.
[31] H. Cui, Y. Qian, H. An, C. Sun, J. Zhai, Q. Li, Electrochemical removal of fluoride from water by PAOA modified carbon felt electrodes in a continuous flow reactor, Water Res., 46 (2012) 3943–3950.
[32] D.S. Bhargava, D.J. Killedar, Fluoride adsorption on fishbone charcoal through a moving media adsorber, Water Res., 26 (1992) 781–788.
[33] C. Janardhana, G.N. Rao, R.S. Sathish, P.S. Kumar, V.A. Kumar, M.V. Madhav, Study on defluoridation of drinking water using zirconium ion impregnated activated charcoals, Indian J. Chem. Technol., 14 (2007) 350–354.
[34] A.K. Gupta, D. Deva, A. Sharma, N. Verma, Adsorptive removal of fluoride by micro-nanohierarchal web of activated carbon fibers, Ind. Eng. Chem. Res., 48 (2009) 9697–9707.
[35] Y. Ma, S.G. Wang, M. Fan, W.X. Gong, B.Y. Gao, Characteristics and defluoridation performance of granular activated carbon coated with manganese oxides, J. Hazard. Mater., 168 (2009) 1140–1146.
[36] M. Karthikeyan, K.P. Elango, Removal of fluoride from aqueous solution using graphite: A kinetic and thermodynamic study, Indian J. Chem. Technol., 15 (2008) 525–532.
[37] V.H. Montoya, L.A.R. Montoya, A.B. Petriciolet, M.A.M. Morán, Optimizing the removal of fluoride from water using new carbons obtained by modification of nut shell with a calcium solution from egg shell, Biochem. Eng. J., 62 (2012) 1–7.
[38] Y. Li, P. Zhang, Q. Du, X. Peng, T. Liu, Z. Wang, Y. Xi, W. Zhang, K. Wang, H. Zhu, D. Wu, Adsorption of fluoride from aqueous solution by grapheme, J. Colloid Interface Sci., 363 (2011) 348–354.
[39] M. Kishore, Y. Hanumantharao, Validation of defluoridation method with "Acacia Arabica" plant by product through 2n factorial experimentation- A statistical approach, Int. J. Appl. Biol. Pharm. Technol., 1 (2010) 1230–1235.
[40] L. Borah, N.C. Dey, Removal of fluoride from low TDS water using low grade coal, Indian J. Chem. Technol., 16 (2009) 361–363.
[41] S. Jagtap, M.K. Yenkie, S. Das, S. Rayalu, Synthesis and characterization of lanthanum impregnated chitosan flakes for fluoride removal in water, Desalination, 273 (2011) 267–275.
[42] M. Ansari, M. Kazemipour, M. Dehghani, M.J. Kazemipour, The defluoridation of drinking water using multi-walled carbon nanotubes, J. Fluorine Chem., 132 (2011) 516–520.
[43] V.S. Rao, C. Chakrapani, C.S. Babu, K.S. Rao, M.N. Rao, D. Sinha, Studies on sorption of fluoride by prepared activated Kaza's carbons, Der. Pharma. Chemica., 3 (2011) 73–83.
[44] V. Martínez-Miranda, J.J. García-Sánchez, M. Solache-Ríos, fluoride ions behavior in the presence of corrosion products of iron: effects of other anions, Sep. Sci. Technol., 46 (2011) 1443–1449.
[45] J.J. García-Sánchez, M. Solache-Ríos, V. Martínez-Miranda, Behavior of fluoride ions in the presence of lanthanum and magnesium modified corrosion products, Sep. Sci. Technol., 50 (2015) 1461–1468.
[46] J.J. García-Sánchez, V. Martínez-Miranda, M. Solache-Ríos, Aluminum and calcium effects on the adsorption of fluoride ions by corrosion Products, J. Fluorine Chem., 145 (2013) 136–140.
[47] P.V.L. Sarin, Snoeyink, D.A. Lytley, W.M. Kriven, Iron corrosion scales. model for scale growth, iron release, and colored water formation, J. Environ. Eng., 130 (2004) 364–373.
[48] B.M. Babić, S.K. Milonjić, M.J. Polovina, B.V. Kaludierović, Point of zero charge and intrinsic equilibrium constants of activated carbon cloth, Carbon, 37 (1999) 477–481.
[49] C. Moreno-Castilla, E. Carrasco-Marin, E. Utrera-Hidalgo, Activated carbons as adsorbents of SO_2 in flowing air. Effect of their pore texture and surface basicity, J. Rivera-Utrilla, Langmuir, 9 (1993) 1378–1383.

[50] F. Guze, The Effect of surface acidity upon the adsorption capacities of activated carbons, Sep. Sci. Technol., 31 (1996) 283–290.
[51] Y.S. Ho, J.C.Y. Ng, G. McKay, Removal of lead(II) from effluents by sorption on peat using second-order kinetics, Sep. Sci. Technol., 36 (2001) 241–261.
[52] R. Liu, W. Gong, H. Lan, Y. Gao, H. Liu, J. Qu, Defluoridation by freshly prepared aluminum hydroxides, Chem. Eng. J., 175 (2011) 144–149.
[53] G. Bitton, Formula Handbook for Environmental Engineers and Scientist, John Wiley & Sons, New York, NY. 1998.
[54] K.J. Farley, D.A. Dzombak, F.M.M. Morel, A surface precipitation model for the sorption of cations on metal oxides, J. Colloid Interface Sci., 106 (1985) 226–242.
[55] J. Lutzenkirchen, Ph. Behra, On the surface precipitation model for cation sorption at the (hydr)oxide water interface, Aquatic Geochem., 1 (1996) 375–397.